On the non-linear energy transfer in a gravity-wave spectrum

Part 3. Evaluation of the energy flux and swell-sea interaction for a Neumann spectrum

By K. HASSELMANN

Institute of Geophysics and Planetary Physics and Department of Oceanography, University of California, La Jolla

(Received 7 August 1962)

The energy transfer due to non-linear interactions between the components of a gravity-wave spectrum discussed in Parts 1 and 2 of this paper is evaluated for a fully and partially developed Neumann spectrum with various spreading factors. The characteristic time scales of the energy transfer are found to be typically of the order of a few hours. In all cases the high frequencies and the low-frequency peak are found to gain energy from an intermediate range of frequencies. The transfer of energy to very low frequencies and to waves travelling at large angles to the main propagation direction of the spectrum is negligible. Computations are presented also for the rate of decay of swell interacting with local wind-generated seas (represented by a Neumann spectrum). An appreciable decay is found only for swell frequencies in the same range as those of the local sea.

1. Computation of the transfer integral

In Part 1 of this paper (Hasselmann 1962) we derived the expression for the energy transfer due to non-linear interactions between the components of a gravity-wave spectrum. Part 2 (1963) was then concerned primarily with the general properties of the transfer equation and, in particular, with its analogy to the Boltzmann equation. We turn now to the more practical problem of evaluating the energy flux for a given ocean wave spectrum in an attempt to assess the role the non-linear transfer process plays in the complete equation for the energy balance of a wind-generated spectrum (Hasselmann 1960). We assume in this part that the ocean is of infinite depth.

Using the simplifications of Part 2, the transfer equation can be written in the form

$$\frac{\partial F(\mathbf{k}_4)}{\partial t} = \int\int\int\int_{-\infty}^{+\infty} \alpha' \delta(\omega_1+\omega_2-\omega_3-\omega_4)\,\omega_4\{\omega_4 F(\mathbf{k}_1)\,F(\mathbf{k}_2)\,F(\mathbf{k}_3) + \omega_3 F(\mathbf{k}_1)\,F(\mathbf{k}_2)F(\mathbf{k}_4) - \omega_1 F(\mathbf{k}_2)\,F(\mathbf{k}_3)\,F(\mathbf{k}_4) - \omega_2 F(\mathbf{k}_1)\,F(\mathbf{k}_3)\,F(\mathbf{k}_4)\}\,d^2k_1\,d^2k_2, \tag{1.1}$$

where

$$\mathbf{k}_3 = \mathbf{k}_1+\mathbf{k}_2-\mathbf{k}_4, \quad \alpha' = \pi\left(\frac{3gD}{2\rho\omega_1\omega_2\omega_3\omega_4}\right)^2, \tag{1.2}$$

and

$$D = D^{+,+,-}_{\mathbf{k}_1,\mathbf{k}_2,-\mathbf{k}_3}$$

as given by equations (4.9), (4.10) of Part 1. It was shown in Part 2 that all four transfer coefficients $D^{+,+,-}_{\mathbf{k}i_1,\mathbf{k}i_2,-\mathbf{k}i_3}$ of a given quadruple interaction are equal.

On account of the δ-function in the integrand, the transfer integral is restricted to the three-dimensional interaction surface

$$\omega_1+\omega_2=\omega_3+\omega_4 \tag{1.3}$$

in $(\mathbf{k}_1, \mathbf{k}_2)$-space. The transformation to the surface integral can be effected most simply by introducing polar co-ordinates k_j, α_j. From (1.2), (1.3) and the relation $\omega_j = (gk_j)^{\frac{1}{2}}$ for infinite-depth gravity waves we obtain

$$2\cos\beta\,|\mathbf{k}_2|\,|\mathbf{k}_1-\mathbf{k}_4| = (\sqrt{k_1}+\sqrt{k_2}-\sqrt{k_4})^4-k_2^2-(\mathbf{k}_1-\mathbf{k}_4)^2, \tag{1.4}$$

where β is the angle between $\mathbf{k}_2$ and $(\mathbf{k}_1-\mathbf{k}_4)$. For fixed k_4, α_4 and given values of k_1, α_1 and k_2, equation (1.4) determines β and hence α_2. We can thus solve for α_2 and express the interaction surface $\omega_1+\omega_2-\omega_3-\omega_4=0$ in the form

$$\alpha_2=\alpha_2(k_1,\alpha_1,k_2).$$

Since the sign of β is not determined by (1.4), the surface has two sheets $\alpha_2^{(1)}$ and $\alpha_2^{(2)}$ corresponding to the values $+\beta$ and $-\beta$. Transforming to the spectral density $f(k,\alpha)=F(\mathbf{k})\,k$ with respect to polar co-ordinates, equation (1.1) can then be written in the form

$$\begin{aligned}\frac{\partial}{\partial t}f(k_4,\alpha_4) = \int_0^\infty\int_0^\infty\int_{-\pi}^{+\pi}\Bigg\{\sum_{j=1}^{2}\omega_4 T\Bigg[&\frac{\omega_4 k_4}{k_3}f(k_1,\alpha_1)f(k_2,\alpha_2^{(j)})f(k_3,\alpha_3^{(j)})\\ &+\omega_3 f(k_1,\alpha_1)f(k_2,\alpha_2^{(j)})f(k_4,\alpha_4)-\omega_2(k_2/k_1)f(k_3,\alpha_3^{(j)})f(k_4,\alpha_4)f(k_1,\alpha_1)\\ &-\omega_1(k_1/k_2)f(k_3,\alpha_3^{(j)})f(k_4,\alpha_4)f(k_2,\alpha_2^{(j)})\Bigg]\Bigg\}d\alpha_1\,dk_1\,dk_2,\end{aligned} \tag{1.5}$$

$$\text{where}\quad T=\begin{cases}\pi\left(\dfrac{3gD}{2\rho\omega_1\omega_2\omega_3\omega_4}\right)^2\dfrac{2\omega_3^3}{k_2\,|\mathbf{k}_1-\mathbf{k}_4|\,|\sin\beta|\,g^2}, & \text{for}\quad |\cos\beta|<1,\\ 0, & \text{for}\quad |\cos\beta|\geqslant 1.\end{cases} \tag{1.6}$$

The function T has, as to be expected, an integrable singularity for $\sin\beta=0$, i.e. along the edge of the projection of the interaction surface on to the (k_1,α_1,k_2)-space. The singularity at $\mathbf{k}_1=\mathbf{k}_4$ is compensated by a zero in the rest of the integrand. In evaluating (1.5) for a series of values k_4 and α_4, some simplification can be achieved by making use of the symmetry and homogeneity of the transfer coefficients. The details need not be given here, however.

The rate of energy transfer was computed for a number of spectra based on Neumann's empirical formula for a fully developed wind-generated spectrum (Pierson, Neumann & James 1955)

$$E_1(\nu)=\frac{30{\cdot}2}{(2\pi\nu)^6}\exp\left\{-2\left(\frac{g}{2\pi\nu v}\right)^2\right\}, \tag{1.7}$$

where $E_1(\nu)$ is the one-dimensional wave-height spectrum in terms of frequency ν (in c/s) and v is the wind-velocity. All quantities are in units of metres and seconds.

The formula (1.7) was chosen from a number of empirical spectra proposed by various authors not so much because it was believed to have more empirical

support than any other, but because (*a*) the spectrum preserves its shape for different wind speeds, so that the influence of the wind is only to change the magnitude and not the form of the energy transfer, and (*b*) the mean square wave slope is finite without having to modify the spectrum at high frequencies. This is desirable since the energy transfer is weighted as the wave slope rather than the wave height.

Equation (1.7) determines only the one-dimensional frequency spectrum. In order to obtain a simple expression for the two-dimensional spectrum $E_2(\nu, \alpha)$ it was assumed that this could be expressed as the product of $E_1(\nu)$ and a frequency-independent spreading factor $S(\alpha)$

$$E_2(\nu, \alpha) = E_1(\nu) S(\alpha), \tag{1.8}$$

where

$$\int_{-\pi}^{+\pi} S(\alpha)\, d\alpha = 1.$$

The relation between E_2 and the energy spectrum $f(k, \alpha)$ is

$$f(k, \alpha) = \frac{\rho g \nu}{2k} E_2(\nu, \alpha).$$

Three spreading factors were considered:

$$S_1(\alpha) = \begin{cases} 8/3\pi \cos^4 \alpha & \text{for } |\alpha| \leqslant \pi, \\ 0 & \text{for } |\alpha| > \pi; \end{cases}$$

$$S_2(\alpha) = \begin{cases} 2/\pi \cos^2 \alpha & \text{for } |\alpha| \leqslant \pi, \\ 0 & \text{for } |\alpha| > \pi; \end{cases}$$

$$S_3(\alpha) = 1/2\pi \quad \text{(isotropic case)}.$$

The first two examples are typical for the spreading factors observed under simple wind conditions. The last example was included as an extreme case for comparison.

Since only the magnitudes but not the shapes of the function E_2 and $\partial E_2/\partial t$ depend on the wind velocity, the computations need to be carried through for one wind-velocity only. Rather than introducing suitable characteristic scales depending on v, we present all results in dimensional form for the wind-velocity $v_0 = 10\,\text{m/s} = 19{\cdot}4\,\text{knots}$, noting that the characteristic frequency ν_c, wave-height ζ_c and interaction time $\tau_c = E_2(\partial E_2/\partial t)^{-1}$ vary with the wind-velocity as

$$\nu_c \sim v^{-1}, \quad \zeta_c \sim v^{\frac{5}{2}}, \quad \tau_c \sim v^{-2}. \tag{1.9}$$

The rates of energy transfer for the spreading factor S_1 are shown, together with the spectra, for three directions $\alpha = 0°$, $30°$ and $60°$ in figure 1. The influence of the spreading factor on the energy transfer for $\alpha = 0°$ is shown in figure 2. The ordinates are adjusted so that the three spectra fall together. Figure 3 shows the rate of transfer for a spectrum still in the stage of growth with a low-frequency cut-off at 0·16 c/s. This corresponds to a wind-duration of approximately 6 h according to Pierson *et al.* (1955). The results should be regarded with some caution in the region where the energy transfer changes rapidly. The ordinate scales in all figures are such that the curve $\partial E_2/\partial t$ represents the amount the spectrum E_2 would change if the energy transfer remained constant at its initial

value over a period of 10^4 sec = 2·8 h. It is seen that even at the moderate wind speed of 10 m/s the non-linear energy transfer is appreciable and will probably have a considerable influence on the energy balance of the spectrum.

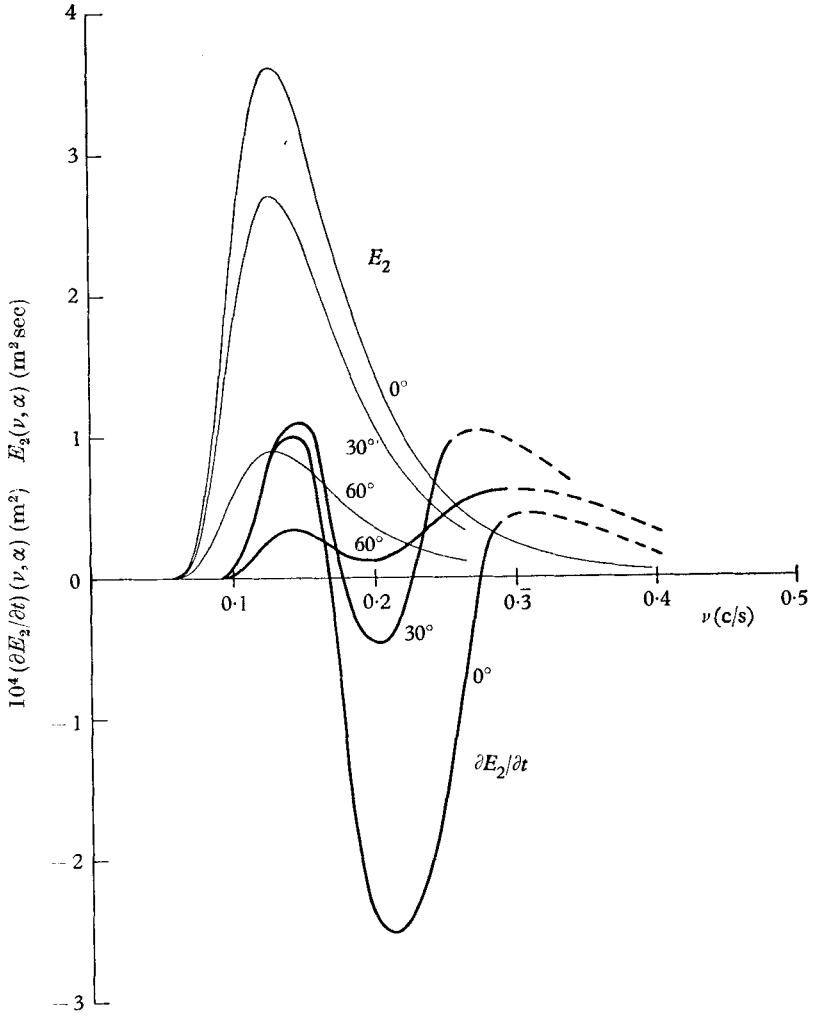

FIGURE 1. Energy transfer for a Neumann spectrum with $\cos^2\alpha$-spreading factor. (Wind velocity: 10 m/s = 19·4 knots.)

The most surprising feature of the energy transfer in all cases is the growth of the peak,† as from the qualitative discussion of Part 1 we should have expected that energy is transferred from the peak to higher wave-numbers. The high wave-numbers do in fact gain energy, as expected, but apparently from the intermediate wave-number range rather than the peak. In a more detailed analysis of the transfer integral later we shall find that a more accurate interpretation is

† In a rough computation of the order of magnitude and direction of the energy flux (Hasselmann 1961), this feature was lost in the numerical scatter. The present computations are otherwise in reasonable agreement with the original ones.

that the high wave-numbers gain energy from both the peak and the intermediate range, the peak gaining energy from the intermediate range more rapidly than it loses energy to the high wave-numbers. It may be pointed out that although very low-energy regions of the spectrum always gain energy, as the dominant

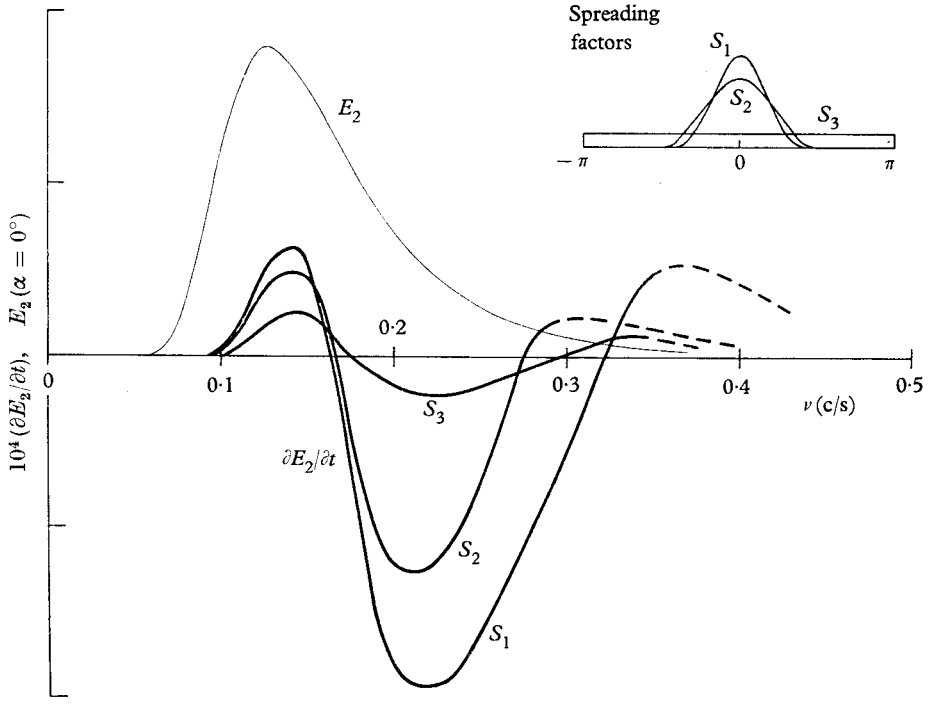

FIGURE 2. Energy transfer for a Neumann spectrum with different spreading factors ($\alpha = 0°$). Ordinate scales are adjusted to give coincident E_2-curves. The ratio $(1/E_2)\,(\partial E_2/\partial t)$ is the same for each spreading factor.

interaction term (the first term in (1.1)) is positive, the converse is not true for a sharp spectral peak since in this case only two of the three dominant interaction terms are negative. The simultaneous energy transfer from the intermediate wave-number range to both lower and higher wave-numbers can be explained to some extent by the fact that the transfer process conserves both the mean energy $\int\int E_2(\nu,\alpha)\,d\nu\,d\alpha$ and the mean 'number density' $\int\int E_2(\nu,\alpha)\,\omega^{-1}\,d\nu\,d\alpha$ (Part 2), since it can be readily seen that it is not possible to conserve both of these moments by a net energy transfer in only one direction.

Another characteristic property of the energy transfer is the extremely weak energy gain at frequencies appreciably smaller than that of the peak. This can be explained by the eighth-power dependence of the transfer coefficient a' on frequency. For this reason it seems improbable that the long-period waves of the white, low-energy regions of the spectra observed by Munk, Miller, Snodgrass & Barber (1963) can be attributed to (non-stationary) non-linear interactions, even if the slightly favourable influence of finite depth is taken into account.

For the spreading factors S_1 and S_2 an extremely small energy flux was also

found for directions greater than 90° to the main propagation direction. The reason for this appears to lie both in the angular dependence of the transfer coefficient and the form of the interaction surface. The back scattering of waves by non-linear energy transfer is thus also generally a negligible effect.

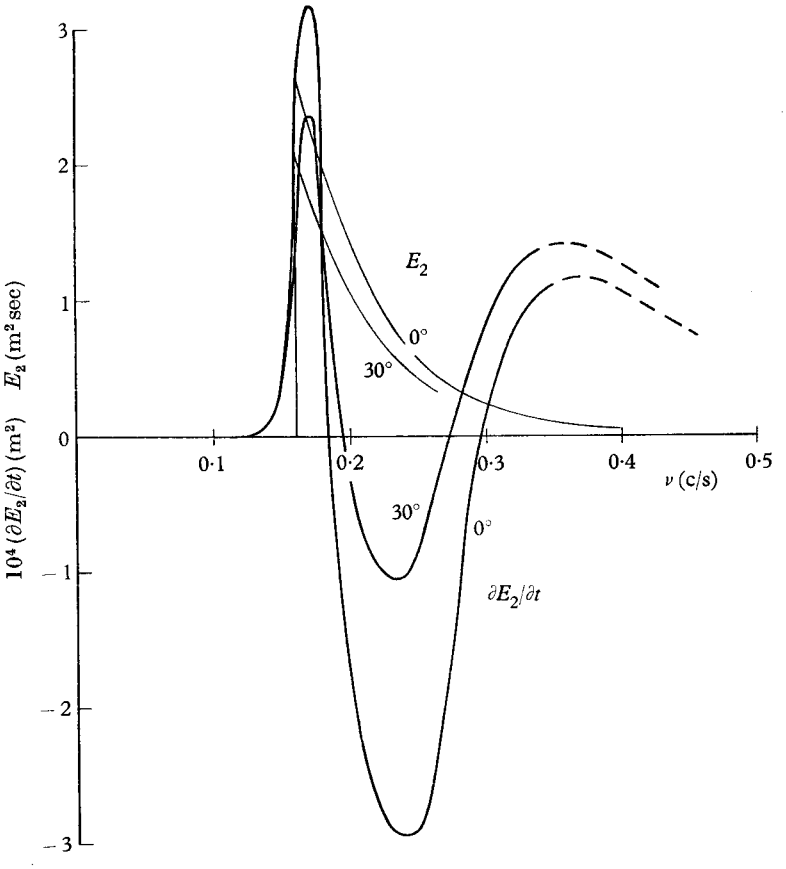

FIGURE 3. Energy transfer for a partially developed Neumann spectrum with $\cos^2\alpha$-spreading factor.

It is found that most of the energy flux is due to interactions involving regions of high energy density near the peak. This explains the increase in energy transfer with decrease in angular spread (figure 2), since a decrease in the angular spread leads to an increase in the maximal spectral density in the mean propagation direction. For very small spreading angles, however, the energy flux must finally decrease again, since in the limiting case of a uni-directional spectrum the flux vanishes (Part 1).

It is of interest to compare the computed non-linear energy flux with the general picture of ocean-wave development as determined by observations and existing theories of wave generation. The observations indicate that shorter waves generally grow at a faster rate than larger waves and also apparently begin to grow *earlier*. This latter feature can be explained by a combination of an

instability theory, such as that of Miles (1957, 1959) and the non-linear energy flux found for a semi-developed spectrum (figure 3). The energy flux to frequencies lower than the cut-off frequency is sufficiently large to trigger an instability mechanism and at the same time is limited to a rather narrow frequency band immediately below the cut-off frequency, so that the longer waves will tend to be generated successively rather than grow simultaneously at different rates. An alternative explanation of the observed successive generation of waves was given by Miles (1960) and Phillips (1961), who assume that the instability mechanism is triggered by an initial wave growth due to random pressure fluctuations (Phillips 1957). At present it is still difficult to assess the relative importance of instability, random-pressure and non-linear energy transfer mechanisms in the development of ocean waves, since quantitative calculations can be carried through for the first process only for laminar boundary layers, and the second process is determined by the three-dimensional pressure spectrum as a function of frequency and wave-number (Hasselmann 1961), about which little is known.

The gain in energy of the spectral peak forces us to accept a rather effective dissipative process at low frequencies (if we assume that for wind-fields of infinite fetch and duration an equilibrium spectrum exists). The only mechanism which suggests itself is wave-breaking, about which, again, very little is known. Possibly, the pronounced peaks of fully developed spectra are determined by the condition that the long waves become sufficiently steep to participate in the wave-breaking process, as was originally implied in the Pierson *et al.* forecasting method.

2. Swell-sea interaction

Apart from their influence on the energy balance of wind-generated spectra, the non-linear interactions may also play an important role in damping swell from distant storms crossing through local wind seas. Formally, the latter problem differs from the former only in the shape assumed for the spectrum; in the first case we considered a smooth spectrum, whereas we shall now consider a swell spectrum $F_s(\mathbf{k})$ consisting of a narrow peak at the wave-number $\mathbf{k}_s$ superimposed on a smooth 'local sea' spectrum $F_l(\mathbf{k})$. If $U = \iint F_s(\mathbf{k})\,dk_1 dk_2$ is then the total energy of the swell, the rate of change of U can be obtained by integrating (1.1) over a small region around $\mathbf{k}_s$:

$$\frac{dU}{dt} = -U\iiiint \pi\left(\frac{3gD}{2\rho\omega_1\omega_2\omega_3\omega_s}\right)^2 \omega_s\{\omega_1 F_l(\mathbf{k}_2)\,F_l(\mathbf{k}_3) + \omega_2 F_l(\mathbf{k}_1)\,F_l(\mathbf{k}_3) - \omega_3 F_l(\mathbf{k}_1)\,F_l(\mathbf{k}_2)\}\,\delta(\omega_1+\omega_2-\omega_3-\omega_s)\,d^2k_1 d^2k_2, \quad (2.1)$$

where $$\omega_s = (gk_s)^{\frac{1}{2}} \quad \text{and} \quad \mathbf{k}_3 = \mathbf{k}_1+\mathbf{k}_2-\mathbf{k}_s.$$

Assuming that the local spectrum remains stationary, the solution to (2.1) is simply

$$U = U_0 e^{-t/\tau}, \quad (2.2)$$

where $1/\tau$ is the integral on the right-hand side of (2.1). The decay time τ depends only on the local sea spectrum and the wave-number $\mathbf{k}_s$ of the swell. A contour

chart showing the dependence of τ on frequency $\nu_s = (2\pi)^{-1}(gk_s)^{\frac{1}{2}}$ and the angle α_s between $\mathbf{k}_s$ and the mean direction of the local sea is shown in figure 4. For the local sea we have again taken Neumann's spectrum with a wind velocity of 10 m/s and the spreading factor S_2. The most characteristic feature is the extremely sharp increase in decay time as the swell frequency falls below the frequency 0·125 c/s of the spectral peak. The non-linear wave coupling thus presents practically no impedance to long-period swell passing through shorter-period local seas. This can again be explained by the 8th power dependence of

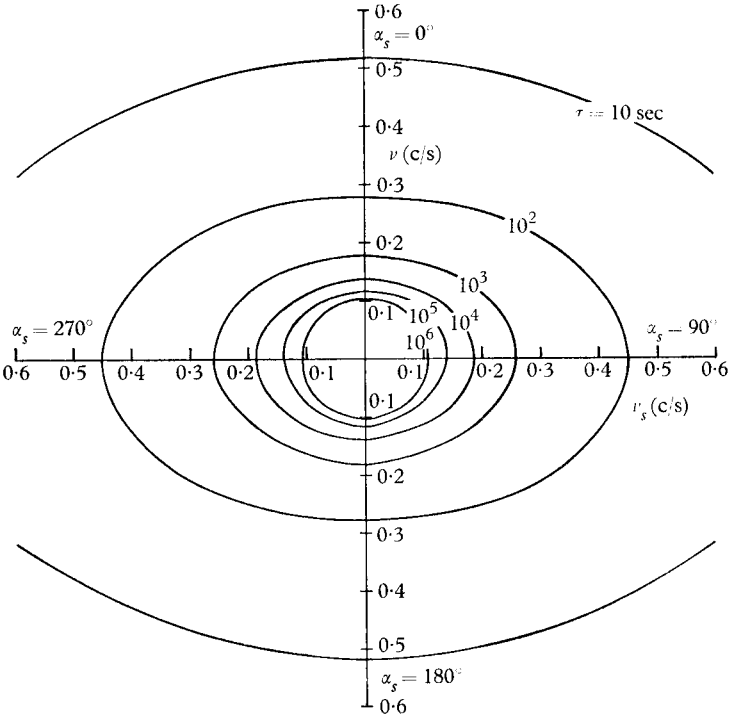

FIGURE 4. Decay time τ for swell travelling through a Neumann spectrum (wind velocity: 10 m/s, spreading factor: $\cos^2\alpha$). The mean direction of the spectrum is upwards ($\alpha_s = 0$); the spectral peak is at 0·125 c/s.

the transfer coefficient on frequency. The qualitative discussion by Munk *et al.* (1963) of a particular interaction which could lead to the damping of swell components of periods appreciably longer than those of the local sea is not pertinent, since the interaction is too weak to produce a measurable effect and is furthermore of the wrong sign.† However, we stress that the continuous energy transfer considered here is only one of the non-linear processes in a random sea. It is possible that wave-breaking could independently cause damping of long-period swell travelling through a local 'saturated' sea.

The dependence of the decay time on the direction of the swell is not pronounced. The damping is slightly smaller for swell travelling at right angles to the local sea than for swell in the same or opposite directions. The influence of

† Unfortunately, the author failed to notice this in an early discussion with Munk.

the spreading factor of the local-sea spectrum is shown in figure 5 for the directions $\alpha_s = 0$ and $\alpha_s = \frac{1}{2}\pi$. The dependence on direction is greater for the smaller angular spread S_1, as expected, the values for the isotropic spectrum lying between the maximum and minimal values of the anisotropic spectra. As will be shown later, the small decay times for high frequencies should be interpreted primarily as a broadening of the swell peak rather than a redistribution of the swell energy over the entire spectrum.

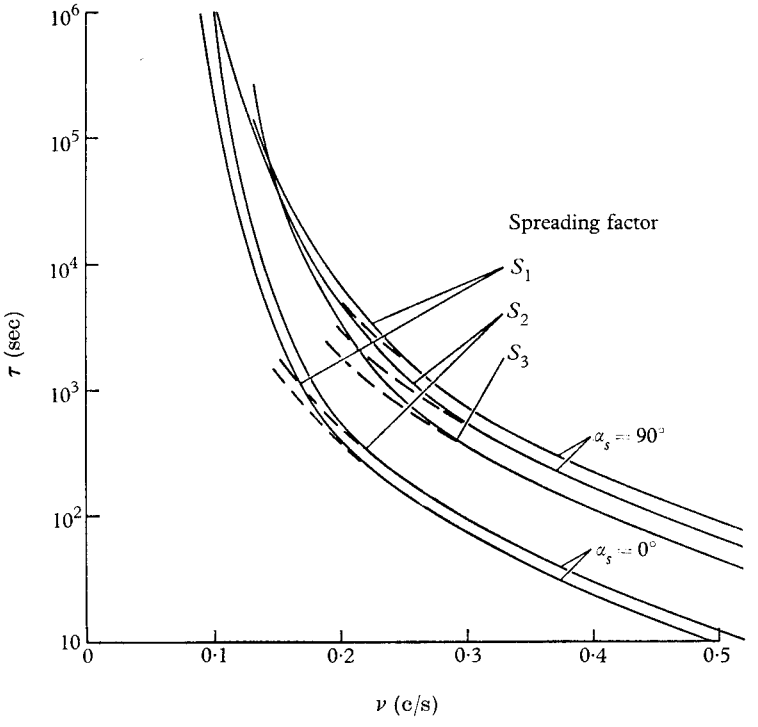

FIGURE 5. Swell decay time τ for different spreading factors of the background spectrum.

Although it does not necessarily follow from (2.1), the value of the decay time τ was found to be positive in all computations, with the possible exception of a narrow frequency range (not shown in figures 4 and 5) just left of the peak of the local sea spectrum in which the integral $1/\tau$ became slightly negative. However, the values of $1/\tau$ in this region represent a very small difference between relatively large contributions to the integral on the right-hand side of (2.1) and the numerical accuracy was probably not sufficient to determine the sign with certainty (in either case, the rate of change of the swell is negligible).

3. Further analysis of the transfer integral

A better understanding of the results of the previous sections can be gained by a more detailed analysis of the transfer integral. Clearly, a representation of the interaction surface $\omega_1 + \omega_2 - \omega_3 - \omega_4 = 0$ for fixed $\mathbf{k}_4$ would be desirable for this purpose. Unfortunately, this meets with some difficulty, as the surface is a

three-dimensional region of a four-dimensional space. However, a geometrical presentation of the set of all possible interaction can be given if we follow a personal suggestion by M. S. Longuet-Higgins and attempt to present not the set of all possible interactions for a given wave-number $\mathbf{k}_4$ (which we should prefer) but rather the set of all wave-number *pairs* $\mathbf{k}_1$ and $\mathbf{k}_2$ interacting with a fixed *pair* $\mathbf{k}_3$, $\mathbf{k}_4$. From the interaction conditions for infinite-depth waves

$$\mathbf{k}_1+\mathbf{k}_2 = \mathbf{k}_3+\mathbf{k}_4 = \mathbf{k}, \tag{3.1}$$

$$\sqrt{k_1}+\sqrt{k_2} = \sqrt{k_3}+\sqrt{k_4} = \sqrt{k\gamma}, \tag{3.2}$$

we obtain $$2\mathbf{k}_1.\mathbf{k} = \mathbf{k}^2+\mathbf{k}_1^2-\mathbf{k}_2^2 = k^2+k_1^2-(\sqrt{k\gamma}-\sqrt{k_1})^4,$$

or, normalizing to $|\mathbf{k}| = 1$ and denoting the angle between $\mathbf{k}_1$ and $\mathbf{k}$ as $\hat{\alpha}_1$,

$$\cos\hat{\alpha}_1 = \frac{1+k_1^2-(\gamma-\sqrt{k_1})^4}{2k_1}. \tag{3.3}$$

For fixed γ, the locus of all wave-numbers $\mathbf{k}_1$ is thus determined by (3.3), the wave-number $\mathbf{k}_2$ then being given by (3.1). The interaction curves for different values of γ are shown in figure 6. Phillips' (1960) interaction curve ($\mathbf{k}_3 = \mathbf{k}_4$) is included as the case $\gamma = \sqrt{2}$. The set of all possible interactions is given by the set of all end points P, P' of the vectors $\mathbf{k}_1$ and $\mathbf{k}_3$, both points lying on the same interaction curve. As suitable parameters determining a given interaction we shall use γ, the abscissae $x_1 = k_1\cos\alpha_1-\frac{1}{2}$ and $x_3 = k_3\cos\alpha_2-\frac{1}{2}$ of the points P and P',† and for cases in which the wave-numbers are not normalized, k.

We consider next the transfer coefficient a'. Since D is a fourth-order homogeneous function of the interacting wave-numbers, a' is of the form

$$a' = \frac{9\pi}{4\rho^2g^2}k^4c,$$

where c is a function of γ, x_1 and x_3. The coefficient c is shown in figure 7 for the two interaction configurations $x_3 = x_1$ and $x_3 = -x_1$. In the first case the points P, P' are coincident, in the second they are symmetrically positioned about the vertical axis of symmetry. For a complete representation of the interaction coefficient, c would need to be plotted for all values of x_3 between $-x_1$ and $+x_1$. (For $|x_3| > |x_1|$ the points P and P' can be interchanged.) However, the general behaviour of c is already apparent from the curves shown. The interactions are seen to be strongest for wave-numbers that lie parallel. This is offset by the fact that at the maximal values of c the points P and P' represent identical wave-number pairs, so that the net energy transfer is balanced (Part 1). The increase of c with γ should be attributed primarily to the choice of normalization, since for large values of γ the interacting wave numbers become large in comparison to the resultant wave-numbers $\mathbf{k}$.

In our computation examples, the dominant interactions appear to have been determined more by the pronounced peak of the spectrum than the behaviour of

† Diagonally opposite points on the interaction chart represent the same wave-number pair. If we limit P and P' to the upper half plane the points are then uniquely determined by x_1 and x_3.

the interaction coefficients. For a given wave-number $\mathbf{k}_4$, the strongest interactions are those involving wave-numbers close to the wave-number $\mathbf{k}_m$ of the spectral peak. Unless $\mathbf{k}_4$ is itself near $\mathbf{k}_m$, not more than two wave-numbers, say $\mathbf{k}_1$ and $\mathbf{k}_3$, can be in the vicinity of $\mathbf{k}_m$ for a given interaction. However, this

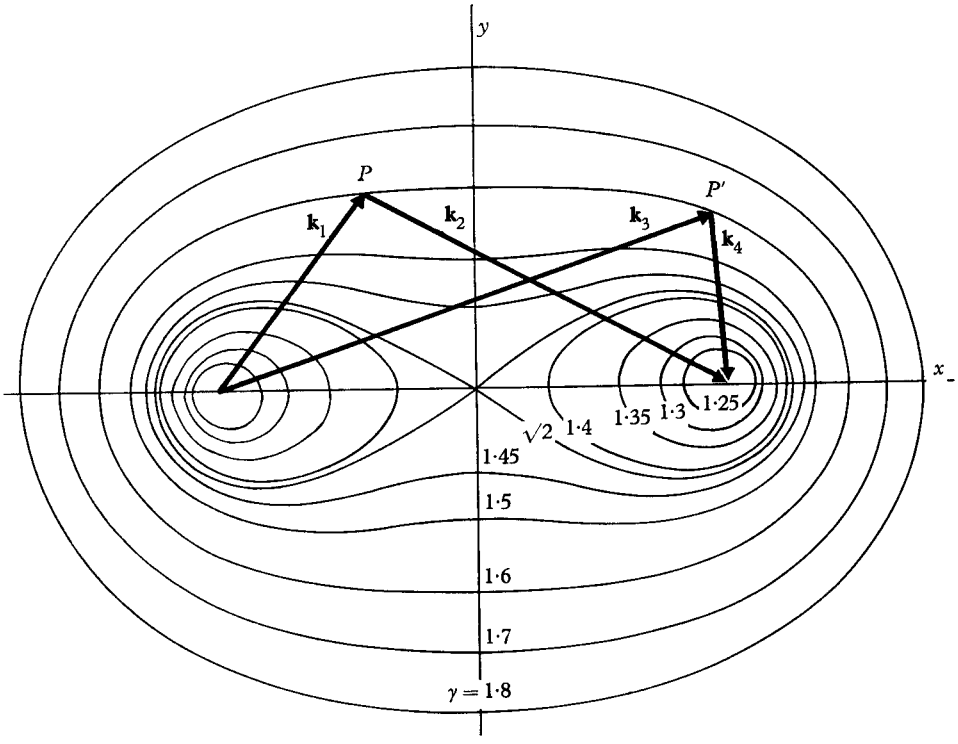

FIGURE 6. Longuet-Higgins's interaction chart. The curve $\gamma = \sqrt{2}$ is Phillips's (1957) 'figure of eight'.

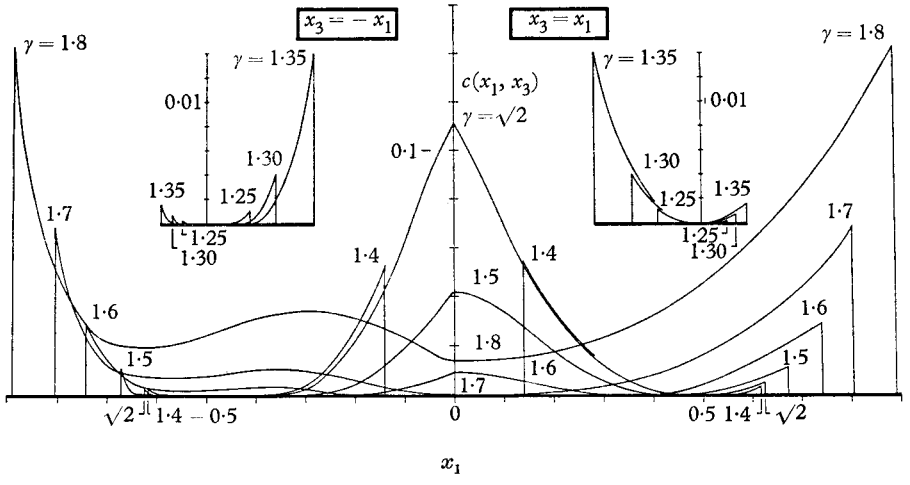

FIGURE 7. The interaction coefficient $c(x_1, x_3, \gamma)$ for the interactions $x_1 = x_3$ $(x_1 \geqslant 0)$ and $x_1 = -x_3$ $(x_1 \leqslant 0)$.

again yields a configuration in which the two wave-number pairs are almost the same, so that the net energy transfer is nearly balanced. Nonetheless, the sharpness of the peak, combined with the behaviour of the interaction coefficients, appeared to outweigh the effect of the factor $\{\ldots\}$ in (1.1) vanishing for equal wave-number pairs, so that the energy transfer was in fact to the greater part due to interactions between almost identical wave-number pairs

$$(\mathbf{k}_1, \mathbf{k}_2) \approx (\mathbf{k}_3, \mathbf{k}_4) \approx (\mathbf{k}_m, \mathbf{k}_4).$$

The situation at the peak itself is rather more complicated and a simple qualitative explanation for the net positive transfer could not be found.† At very high or very low wave-numbers the coupling with the peak dominates completely. In this case our qualitative description can be formulated more rigorously in the form of an asymptotic expansion.

4. Asymptotic expansions

For large wave-numbers $\mathbf{k}_4$, the net energy change $(\partial F(\mathbf{k}_4)/\partial t)$ can be considered to consist of two parts: the transfer $(\partial F(\mathbf{k}_4)/\partial t)_1$ due to all interactions with wave-numbers $\mathbf{k}_j$ greater than ϵk_4, where ϵ is a small but fixed quantity, and the remaining transfer $(\partial F(\mathbf{k}_4)/\partial t)_2$ due to interactions involving at least one wave-number smaller than ϵk_4. For sufficiently large k_4, the first set of interactions will exclude all wave-numbers contributing appreciably to the mean energy, or any other finite moment of the spectrum.

In order to obtain an estimate for $(\partial F(\mathbf{k}_4)/\partial t)_1$, we assume that the spectrum preserves its form asymptotically, i.e. for $k > \epsilon k_4$ and sufficiently large $\mathbf{k}_4$,

$$F(\mathbf{k}) = F(\mathbf{k}_4)\, \eta(\mathbf{k}_4)\, \psi(k[k_4 \xi(k_4)]^{-1}). \tag{4.1}$$

This is the case, for instance, if the spectrum falls off exponentially or as a power of k. From (1.1) we then find

$$\left(\frac{\partial F(\mathbf{k}_4)}{\partial t}\right)_1 = \text{const.}\, g^{-\frac{3}{2}} \rho^{-2} (k_4 \xi(k_4))^{\frac{17}{2}} \{F(\mathbf{k}_4)\, \eta(k_4)\}^3. \tag{4.2}$$

The evaluation of $(\partial F(\mathbf{k}_4)/t)_2$ requires a more detailed analysis of the interaction surface and transfer coefficients. According to figure 6, interactions between wave-numbers of appreciably different magnitudes are possible only for values of γ very near to 1: $\gamma = 1 + \sqrt{r}$ $(r \ll 1)$. Of the wave-numbers $\mathbf{k}_1$ and $\mathbf{k}_2$, one, say $\mathbf{k}_2$, is then approximately equal to $\mathbf{k}_4$. By expanding the interaction equations it can further be shown that the interaction curves are almost circles with centres at $-\frac{1}{2}$ and $+\frac{1}{2}$, so that $k_1 \approx k_3 \approx rk$ or, more precisely,

$$k_1 = rk\left[1 + \left(\frac{r}{k}\right)^{\frac{1}{2}} \cos\hat{\alpha}_1 + \ldots\right],$$

$$k_3 = rk\left[1 + \left(\frac{r}{k}\right)^{\frac{1}{2}} \cos\hat{\alpha}_3 + \ldots\right],$$

† The growth of the peak suggests the possibility that very narrow peaks tend generally to develop into δ-functions. An investigation of this point, however, led to the result that extremely narrow peaks tend to flatten, so that the growth of the peak in our case is due to the coupling of the peak to the rest of the spectrum (see also Part 2).

where $k = |\mathbf{k}_1 + \mathbf{k}_2| = |\mathbf{k}_3 + \mathbf{k}_4|$ and $\hat{\alpha}_j$ is the angle between $\mathbf{k}_j$ and $\mathbf{k}$. Expanding the transfer coefficient c for small values of r then yields

$$c = \frac{r^3}{9}\{(\cos\hat{\alpha}_1 + \cos\hat{\alpha}_3)[1 + \cos(\hat{\alpha}_1 - \hat{\alpha}_3)]\}^2 + \ldots.$$

If we assume that the spectrum at $\mathbf{k}_2$ or $\mathbf{k}_4$ is appreciably smaller than at $\mathbf{k}_1$ or $\mathbf{k}_3$, the expression $\{\ldots\}$ in (1.1) can be expanded also in terms of the derivatives of the spectrum at $\mathbf{k}_4$,

$$\omega_4 F_1 F_2 F_3 + \omega_3 F_1 F_2 F_4 - \omega_2 F_1 F_3 F_4 - \omega_1 F_2 F_3 F_4 = F_1 F_3 \{\omega_4 \nabla F_4 - F_4 \nabla \omega_4\}(\mathbf{k}_2 - \mathbf{k}_4) + \ldots.$$

By substituting these expansions in (1.1), transforming to the integration variables k_1, α_1, k_3, α_3 and eliminating k_3 by the interaction condition

$$\omega_1 + \omega_2 - \omega_3 - \omega_4 = 0,$$

it can then be shown that

$$\left(\frac{\partial F(\mathbf{k}_4)}{\partial t}\right)_2 = O\{F(\mathbf{k}_4)\} g^{-\frac{3}{2}} \rho^{-2} \int_0^\infty dk_1 k_1^{\frac{11}{2}} \int\int_{-\pi}^{+\pi} d\alpha_1 d\alpha_3 f(k_1, \alpha_1) f(k_1, \alpha_3) Q(\alpha_1, \alpha_3), \tag{4.3}$$

where $f(k, \alpha) = kF(\mathbf{k})$ is the spectral density in polar co-ordinates and Q is a trigonometrical function of the angles α_1, α_3. The expression $O\{F(\mathbf{k}_4)\}$ depends on derivatives of $F(\mathbf{k}_4)$ up to the second order. It has been assumed that $k_i(\partial F/\partial k_j)$ and $k_i k_j(\partial^2 F/\partial k_l k_m)$ are of the same order as F or smaller.

To compare the two contributions (4.2) and (4.3), we assume for simplicity that F is proportional asymptotically to some power, $-q$, of k. The scale factors ξ and η in (4.1) are then constant, and (4.2) becomes

$$\left(\frac{\partial F(\mathbf{k}_4)}{\partial t}\right)_1 = O(k_4^{\frac{17}{2} - 3q}),$$

whereas from (4.3)

$$\left(\frac{\partial F(\mathbf{k}_4)}{\partial t}\right)_2 = O(k_4^{-q}).$$

Hence for large k_4, $(\partial F(\mathbf{k}_4)/\partial t)_2$ is great or small in comparison to $(\partial F(\mathbf{k}_4)/\partial t)_1$ according as q is greater or smaller than 4·25. The integral in (4.3) converges only if $q > 4{\cdot}25$, which is consistent with this result.

For a Neumann spectrum, $q = 4{\cdot}5$, so that the energy gain at high wave-numbers in figures 1–3 is due predominately to interactions with the peak. The net energy gain at the peak must hence be due to interactions of the peak with intermediate wave-numbers, the latter losing energy to both lower and higher wave-numbers.

For $q < 4{\cdot}25$ the energy transfer at high wave-numbers is predominantly local. For small q the question then arises whether the transfer integral is still convergent. By carrying through the corresponding expansion for interactions between $\mathbf{k}_4$ and wave-numbers large in comparison to $\mathbf{k}_4$ it can be shown that the transfer integral generally converges if $F(\mathbf{k})\sqrt{k}$ is integrable. Since this corresponds to a moment of the same order as the mean momentum, the transfer integral is presumably always convergent for real spectra.

The asymptotic expansion for the decay time of a 'swell' peak of very short period superimposed on a continuous background spectrum $F_l(\mathbf{k})$ can be derived in the same way as above. For the decay time τ_1 due to interactions with wave-numbers of the same order of magnitude as the swell wave-number $\mathbf{k}_s$ one finds

$$\tau_1^{-1} = \text{const.}\, g^{-\frac{3}{2}}\rho^{-2}\{k_s\xi(k_s)\}^{\frac{17}{2}} F_l^2(\mathbf{k}_s)\,\eta^3(k_s), \tag{4.4}$$

and for the decay time τ_2 due to interactions with the energy-containing range

$$\tau_2^{-1} = \frac{\pi g^{-\frac{3}{2}}k_4^2}{\zeta^2}\int_0^\infty dk_1\, k_1^{\frac{7}{2}}\int\int_{-\pi}^{+\pi} f(k_1,\alpha_1)f(k_1,\alpha_3)\,(\cos\alpha_1+\cos\alpha_3)^2 \times[1+\cos(\alpha_1-\alpha_3)]^2\, d\alpha_1 d\alpha_3. \tag{4.5}$$

Hence in this case the interactions with the energy-containing range dominate if q is greater than only 3·25. The greater part of the swell energy is transferred by these interactions from the wave-number $\mathbf{k}_s$ $(=\mathbf{k}_4)$ via two relatively small wave-numbers $\mathbf{k}_1$ and $\mathbf{k}_3$ to a resultant wave-number $\mathbf{k}_2 = \mathbf{k}_3+\mathbf{k}_4-\mathbf{k}_1$ which is still close to $\mathbf{k}_4$. Thus for large $\mathbf{k}_s$ the 'swell' decay should be interpreted primarily as a broadening of the swell peak rather than a genuine damping. The asymptotic values of τ_2 as given by (4.5) are shown in figure 5. The agreement between the asymptotic and computed curves is good for $\nu > 0{\cdot}2$ c/s.

Asymptotic expressions for τ were evaluated further for swell periods which were long in comparison to those of the background spectrum. The decay times were found to be extremely large and varied as the -11th power of ν_s, in consistence with the sharp increase of the computed values of τ at low frequencies.

REFERENCES

Hasselmann, K. 1960 *Schiffstechnik*, **7**, 191–5.

Hasselmann, K. 1961 *Proc. Conf. Ocean Wave Spectra*, Easton, Md. (in the Press).

Hasselmann, K. 1962 *J. Fluid Mech.* **12**, 481–500.

Hasselmann, K. 1963 *J. Fluid Mech.* **15**, 273–281.

Miles, J. W. 1957 *J. Fluid Mech.* **3**, 185–204.

Miles, J. W. 1959 *J. Fluid Mech.* **6**, 568–82, 583–98.

Miles, J. W. 1960 *J. Fluid Mech.* **7**, 469–78.

Munk, W. H., Miller, G., Snodgrass, F. E. & Barber, N. F. 1963 *Phil. Trans.* (in the Press).

Phillips, O. M. 1957 *J. Fluid Mech.* **2**, 417–45.

Phillips, O. M. 1960 *J. Fluid Mech.* **9**, 193–217.

Phillips, O. M. 1961 *Proc. Conf. Ocean Wave Spectra*, Easton, Md. (in the Press).

Pierson, W. J., Neumann, G. & James, R. W. 1955 *U.S. Navy Dept. Hydrog. Off.* (*Wash.*), Publ. no. 603.